THE ASTRONOMICAL JOURNAL, 117:562–573, 1999 January

THE NEARBY LOW-MASS VISUAL BINARY WOLF 424[1]

GUILLERMO TORRES AND TODD J. HENRY
Harvard-Smithsonian Center for Astrophysics, 60 Garden Street, Cambridge, MA 02138; gtorres@cfa.harvard.edu, thenry@cfa.harvard.edu
AND
OTTO G. FRANZ AND LAWRENCE H. WASSERMAN
Lowell Observatory, 1400 West Mars Hill Road, Flagstaff, AZ 86001; ogf@lowell.edu, lhw@lowell.edu
Received 1998 August 31; accepted 1998 September 16

ABSTRACT

We present new measurements of the relative positions of the components of the low-mass visual binary Wolf 424 (M5.5 Ve) made with the Fine Guidance Sensors on the *Hubble Space Telescope*. Previous analyses of the astrometric orbit of this system indicated that the components have substellar masses (Heintz; Schultz et al.), raising considerable interest as the first candidate brown dwarfs to have their masses measured dynamically. These studies relied partly on visual and photographic measurements, which are affected by systematic errors in the angular separation and have thus biased those solutions. Our new orbital solution using only the position angles of the early measurements together with all available modern high-resolution observations including our own shows that the component masses are clearly above the substellar limit ($M_A = 0.143 \pm 0.011\ M_\odot$, $M_B = 0.131 \pm 0.010\ M_\odot$), and thus they are *not* brown dwarfs. Recent evolutionary models for low-mass stars show good agreement with the location of Wolf 424A and B in the mass-luminosity diagram in the K band. In addition, we show that while the secondary appears to have normal colors compared to similar M dwarfs, the primary star is fainter than expected at optical wavelengths (B, V), possibly owing to significant spot coverage. This is consistent with the strong flaring activity displayed by the system.

Key words: binaries: visual — stars: fundamental parameters — stars: individual (Wolf 424) — stars: low-mass, brown dwarfs

1. INTRODUCTION

The nearby visual binary Wolf 424 (also known as Gliese 473, FL Vir, and LHS 333, among other designations; $\alpha = 12^h33^m17^s.4$, $\delta = +9°01'16''$, epoch and equinox J2000) has attracted considerable attention over the past several years in connection with claims that both of its components have masses below the substellar limit ($M \approx 0.08\ M_\odot$). The published estimates range from $M \sim 0.05\ M_\odot$ to $0.07\ M_\odot$ (Heintz 1972, 1989; Schultz et al. 1998). This places them in the brown dwarf regime, where the central temperature is too low to ignite hydrogen fusion, and the objects therefore never reach the main sequence. A great deal of modeling effort over the past few years has resulted in a much better theoretical understanding of these objects (see, e.g., Saumon, Chabrier, & van Horn 1995; Marley et al. 1996; Allard et al. 1997; Burrows et al. 1997). The discovery of examples with directly measured masses in this range would be very important for a comparison with detailed evolutionary calculations.

Wolf 424 is composed of two late-type M dwarfs of nearly equal brightness (combined spectral type M5.5 Ve), with a maximum angular separation of about 1″. It is also a flare star (see, e.g., Moffet 1973). Its binary nature was discovered from the elongation of the blended photographic images (Reuyl 1938, 1941), and the importance of the object for the extension of the stellar mass-luminosity relation (MLR) toward lower masses was recognized immediately (Kuiper 1938). The first orbital solution was published by Heintz (1972), giving a period of 16.2 yr and a semimajor axis of 0″.76, and was based partly on difficult measurements of elongated photographic images and also on a few visual measurements. Subsequent revisions of these elements (Heintz 1989, 1993) changed only the semimajor axis and the period slightly.

With the advent of the speckle technique, the system was followed by several groups with considerably higher precision, both in the visual band and at infrared wavelengths. These measurements seem to disagree with the predicted positions (Henry et al. 1992), which suggests that the semimajor axis may need revision, although this conclusion has not been universally accepted (Heintz 1993, 1994). In the meantime, claims have appeared that the apparent discrepancies might be resolved if the orbital period were considerably shorter than 16 yr (Perrier et al. 1992), possibly as short as 8 yr. With this, the masses would be substantially larger, and the components would no longer be brown dwarfs.

More recently, Schultz et al. (1998) carried out a reanalysis of the existing positional information along with their new measurement of Wolf 424 made with the imaging mode of the *Hubble Space Telescope* Faint Object Spectrograph (*HST*/FOS). Their preferred orbital solution, with a period of 15.2 yr and a semimajor axis $a = 0''.747$, leads to a total mass of $0.143\ M_\odot$ using the known parallax of the system, and yielded component masses of $\sim 0.07\ M_\odot$, just under the theoretical limit for a brown dwarf. As with prior solutions, the semimajor axis of their orbit is determined to some extent by the visual and photographic measures, as a result of the adopted weighting scheme. An alternate solution using only the speckle and *HST* observations gave a significantly larger semimajor axis ($a = 0''.907$) and a total mass of $0.232\ M_\odot$ but was considered less satisfactory.

Thus, the components of Wolf 424 are currently still

[1] Based in part on observations with the NASA/ESA *Hubble Space Telescope*, obtained at the Space Telescope Science Institute, which is operated by the Association of Universities for Research in Astronomy, Inc., under NASA contract NAS 5-26555.

regarded as promising brown dwarf candidates, the first to have their masses measured dynamically.

Such small masses, however, are difficult to reconcile with other photometric and spectroscopic evidence. Based on his own mass determinations (0.059 and 0.051 $M_\odot$ for Wolf 424 A and B, respectively), Heintz (1989) pointed out that the components appear to be more than a magnitude above the extrapolated MLR for red dwarfs. This was shown also by Henry et al. (1992) (their Fig. 4), who inferred considerably larger photometric masses of 0.13 and 0.12 $M_\odot$ for the two stars using an updated empirical MLR. Davidge & Boeshaar (1991) examined various gravity-sensitive absorption features in a near-infrared (2 μm) spectrum of Wolf 424 and compared them with the same features in Gliese 65AB and Gliese 866AB, two very similar M dwarf systems. They concluded that the masses of the components of Wolf 424 are unlikely to be under $\sim 0.06\ M_\odot$, although they could not rule this out conclusively. Similarly, Henry et al. (1992) showed that the red spectrum of Wolf 424 is virtually indistinguishable from that of Gliese 65A, which is known to have a mass that is clearly above the hydrogen-burning limit ($M = 0.102 \pm 0.010\ M_\odot$ using data in Henry & McCarthy 1993 and the best available parallax of $\pi_{\rm trig} = 0''.3732 \pm 0''.0027$ by van Altena, Lee, & Hoffleit 1995).

If substellar masses are assumed, the photometric and spectroscopic properties of Wolf 424A and B can be understood only if the system is extremely young (<0.1 Gyr), so that the components have not yet cooled. Although not impossible, Davidge & Boeshaar (1991) considered this possibility rather unlikely. In addition, if the masses are truly substellar (and smaller than 0.06 $M_\odot$), the objects should have preserved their initial lithium content because their central temperature would be too low to deplete this element. Magazzù, Martín, & Rebolo (1993) find, however, that the present Li abundance in Wolf 424 is at least 4 orders of magnitude below the cosmic level and is similar to that determined for Gliese 65A. The implication, again, is that the masses must be above $\sim 0.06\ M_\odot$.

The confusing state of affairs regarding the true nature of Wolf 424 has motivated us to obtain new and more precise measurements of the relative positions of the binary components using the Fine Guidance Sensors (FGS) on *HST*, which can measure angular separations accurate to a few milliarcseconds. We now have four observations of the secondary as it approaches apastron that complement the speckle measurements taken half an orbit earlier. When combined, these data strongly constrain the semimajor axis, the key element for determining the masses.

With these new measurements we carry out a new determination of the orbital elements incorporating all available observations of the pair. The visual and photographic data that have played a crucial role in previous analyses are examined carefully for systematic errors and are included selectively to provide a more balanced and unbiased solution. We show that Wolf 424A and B clearly have stellar masses, which are consistent with all of the spectroscopic and photometric data. In addition, we uncover color anomalies in the primary star possibly related to the flaring activity.

2. OBSERVATIONS

A variety of astrometric observations of different kinds and of different quality have been collected for Wolf 424 over the years. A judicious combination of these data into a balanced orbital solution requires an understanding of the uncertainties and possible biases of each type of observation, since the result in this particular case depends to a large degree on how they are weighted. Clear evidence of this is seen in the work by Schultz et al. (1998), especially regarding the size of the orbit. For this reason we believe a few comments on these data are in order.

2.1. *Photographic, Visual, and Speckle Measurements from the Literature*

Because of its large parallax ($\pi_{\rm trig} \simeq 0''.23$) and proper motion ($\mu \simeq 1''.8\ {\rm yr}^{-1}$), Wolf 424 was recognized as an important target by the 1930s and was followed photographically for several decades in an effort to refine those quantities, principally at the Van Vleck, Sproul, and Leander McCormick observatories. The components of the pair are of similar brightness, and the images on the plates are in many cases elongated, which is how the binary nature was discovered. The elongations on the Sproul and McCormick plates were subsequently measured and converted to angular separations (ρ) and position angles (θ) (see Reuyl 1938; Heintz 1972). Empirical corrections were applied to the separations in an to attempt to compensate for guiding errors, as described by Heintz (1972). These difficult measurements are at the limit of what is possible with the photographic technique and are published as "normal" places by averaging together up to a dozen or more plates typically with several exposures each. The plate series cover an interval of about 50 yr and are thus valuable especially for determining the orbital period of the system. Occasionally the photographic images show no measurable elongation, yet even those instances are useful as checks on the orbital solution (see § 3) and in fact were crucial for the early estimates of the period.

Visual measurements with a filar micrometer have also been made sporadically by several observers, although because of the faintness of the components ($V \approx 13.2$), they are also very difficult and often discordant.

Speckle measurements of the pair in the infrared started in 1983 (Henry et al. 1992) and have continued since by several groups both in the visual (Blazit, Bonneau, & Foy 1987; Balega et al. 1994) and in the infrared (Perrier et al. 1992). Four of the early measurements by Henry et al. are one-dimensional (made in the north-south direction only) but are useful for the information they contain on the semimajor axis because they were made near apastron. Although they have not been included explicitly in previous orbital solutions, we will do so in § 3. Finally, an infrared speckle measurement recently published by Carbillet et al. (1996) is apparently a rereduction of one of the observations by Perrier et al. (1992) with a different technique, and we will assume that it supersedes the original measurement.

A listing including most of the photographic, visual, and speckle measurements of Wolf 424 from the Washington Double Star Catalog[2] (Worley & Douglass 1996) was kindly provided to us by Charles E. Worley. Additional measurements were added from the recent literature. The uncertainties of all these observations are discussed in § 3, and the measurements are listed in Table 1.

[2] Available on-line at http://aries.usno.navy.mil:80/ad_home/wds/.

TABLE 1

ASTROMETRIC OBSERVATIONS OF WOLF 424

Date	θ (deg)	ρ (arcsec)	Type[b]	References	$(O-C)_\theta$ (deg)	$(O-C)_\rho$ (arcsec)	$(O-C)_\theta$ (σ_θ)	$(O-C)_\rho$ (σ_ρ)	Orbital Phase[d]
1938.34	321.7	0.72	Phot	1	−2.37	(−0.470)	−0.31	(−4.89)	0.551
1938.38	312.[a]	1.0	Vis	2	−11.95	(−0.189)	−2.17	(−1.97)	0.553
1938.42	321.3[a]	1.10	Vis	3	−2.53	(−0.088)	−0.51	(−0.92)	0.556
1939.18	316.1	0.81	Phot	1	−5.39	(−0.340)	−0.79	(−3.54)	0.604
1940.16	311.4	0.73	Phot	1	−6.61	(−0.294)	−0.88	(−3.06)	0.667
1941.18	300.3	0.29	Phot	1	−12.52	(−0.511)	−0.66	(−5.32)	0.732
1941.44	239.	0.4	Vis	4	(−71.94)	(−0.330)	(−5.23)	(−3.43)	0.749
1941.51	260.	0.15	Vis	4	−50.37	(−0.560)	−1.37	(−5.83)	0.753
1946.20	126.4	0.45	Phot	1	−11.69	(−0.181)	−0.96	(−1.88)	1.053
1950.13	335.6	0.70	Phot	1	−6.32	(+0.064)	−0.80	(+0.67)	1.304
1952.29	325.0[a]	0.80	Vis	4	−4.42	(−0.285)	−0.64	(−2.97)	1.443
1952.37	326.3	0.69	Phot	1	−2.84	(−0.406)	−0.36	(−4.23)	1.448
1952.53	294.2[a]	0.51	Vis	5	(−34.38)	(−0.604)	(−3.19)	(−6.30)	1.458
1953.21	323.8	0.68	Phot	1	−2.59	(−0.492)	−0.32	(−5.12)	1.501
1954.15	316.7	0.73	Phot	1	−6.85	(−0.457)	−0.91	(−4.76)	1.561
1955.38	338.7	0.73	Phot	1	+19.10	(−0.359)	+2.54	(−3.74)	1.640
1956.17	316.9	0.43	Phot	1	+0.49	(−0.524)	+0.04	(−5.46)	1.691
1956.33	315.8[a]	0.44	Vis	4	+0.17	(−0.480)	+0.01	(−5.00)	1.701
1960.30	169.3	0.8	Vis	6	+13.70	(+0.301)	+1.99	(+3.13)	1.955
1962.22	140.	1.5	Phot	7	+6.31	(+0.928)	+0.86	(+9.67)	2.077
1965.176	353.1[a]	0.37	Vis	8	+2.68	(−0.096)	+0.18	(−1.00)	2.266
1965.40	0.	0.2	Phot	1	+13.41	(−0.331)	+0.49	(−3.45)	2.281
1966.29	343.5	0.56	Phot	1	+6.05	(−0.211)	+0.62	(−2.20)	2.337
1967.18	329.2	0.72	Phot	1	−3.24	(−0.245)	−0.42	(−2.55)	2.394
1968.20	326.9	0.73	Phot	1	−1.58	(−0.387)	−0.21	(−4.04)	2.460
1968.34	336.6[a]	0.75	Vis	9	+8.59	(−0.382)	+1.17	(−3.98)	2.469
1969.16	328.6	0.77	Phot	1	+3.16	(−0.415)	+0.44	(−4.32)	2.521
1970.32	324.5	0.84	Phot	1	+2.57	(−0.321)	+0.39	(−3.35)	2.595
1970.46	323.1	0.73	Vis	10	+1.62	(−0.421)	+0.21	(−4.38)	2.604
1971.30	320.2	0.68	Phot	1	+1.64	(−0.368)	+0.20	(−3.84)	2.658
1979.18	125.8	0.35	Phot	11	+31.00	(+0.100)	+1.97	(+1.04)	3.161
1983.485	...	0.818[c]	Sp	12	...	−0.109	...	−1.33	3.437
1984.356	...	0.902[c]	Sp	12	...	−0.071	...	−0.79	3.492
1984.50	324.0	0.87	Phot	11	−2.35	(−0.302)	−0.37	(−3.14)	3.502
1985.32	330.8	0.86	Vis	11	+6.92	(−0.329)	+1.08	(−3.43)	3.554
1986.4499.....	322.7[a]	1.098	Sp	13	+2.37	−0.018	+1.18	−0.41	3.626
1987.72	312.8	0.81	Phot	11	−2.28	(−0.087)	−0.34	(−0.91)	3.707
1989.219	...	0.196[c]	Sp	12	...	−0.039	...	−1.97	3.803
1989.219	...	0.184[c]	Sp	12	...	−0.051	...	−2.75	3.803
1989.39	304.9	0.30	Vis	14	+8.35	(−0.107)	+0.46	(−1.11)	3.814
1990.0400.....	278.0	0.220	Sp	15	+15.11	+0.010	+3.03	+0.88	3.856
1990.181	248.	0.179	Sp	12	+0.52	−0.007	+0.26	−1.03	3.865
1990.183	246.	0.177	Sp	12	−1.23	−0.009	−0.62	−1.29	3.865
1990.359	226.	0.177	Sp	12	+1.75	−0.002	+0.87	−0.26	3.876
1990.4399.....	210.5	0.186	Sp	15	−3.32	+0.001	−0.67	+0.12	3.881
1991.17	197.4	0.18	Vis	16	+32.51	(−0.197)	+1.06	(−2.05)	3.928
1991.237	160.	0.430	Sp	17	−2.99	+0.033	−0.60	+2.17	3.932
1991.320	164.	0.343	Sp	12	+3.10	(−0.080)	+1.55	(−5.82)	3.938
1991.323	164.	0.374	Sp	12	+3.17	(−0.050)	+1.58	(−3.33)	3.938
1991.422	161.6	0.436	Sp	12	+2.96	−0.017	+1.48	−0.99	3.944
1993.3514.....	135.8	0.602	Sp	18	+0.23	+0.002	+0.11	+0.10	4.067
1995.5733.....	26.04	0.2359	FGS	19	−0.53	+0.001	−1.28	+1.09	4.209
1996.2923.....	353.2	0.416	FOS	20	−0.90	−0.001	−0.36	−0.04	4.255
1996.4606.....	350.53	0.4639	FGS	19	+0.10	−0.002	+0.48	−1.64	4.266
1997.4341.....	338.44	0.7344	FGS	19	−0.05	−0.001	−0.39	−0.69	4.328
1998.2510.....	333.46	0.9245	FGS	19	+0.03	+0.001	+0.24	+1.23	4.381

[a] Quadrant reversed from published value.

[b] Phot = photographic; Vis = visual; Sp = one- or two-dimensional speckle; FGS = *HST* Fine Guidance Sensors; FOS = HST Faint Object Spectrograph (imaging mode).

[c] North-south separation.

[d] Integer part counts cycles from periastron passage prior to first observation.

REFERENCES.—(1) Heintz 1972; (2) Reuyl 1938; (3) Kuiper 1938; (4) Worley & Douglass 1996; (5) Wilson 1954; (6) Worley 1962; (7) Luyten 1969; (8) Worley 1972; (9) Couteau 1970; (10) van Biesbroeck 1975; (11) Heintz 1989; (12) Henry et al. 1992; (13) Blazit et al. 1987; (14) Heintz 1990; (15) Perrier et al. 1992; (16) Heintz 1993; (17) Carbillet et al. 1996; (18) Balega et al. 1994; (19) This paper; (20) Schultz et al. 1998.

2.2. *HST Observations*

Four *HST* FGS3 observations of Wolf 424 have been made during the last 3 yr under *HST* observing programs GO 6047, GO 6566, and GO 7493. *HST* FGS3, the "astrometry" Fine Guidance Sensor, was used in transfer function scan mode (TRANS) to measure the component separation, position angle, and brightness difference through filter F583W (central wavelength = 5830 Å) at each epoch. Details on observing with FGS3 in TRANS mode can be found in Franz et al. (1992) and in the FGS Instrument Handbook. The number of TRANS scans in a visit was decreased from 62 to 26 and the scan length gradually increased from 0.″8 to 3.″0 along each scan axis as the companion moved farther from the primary. These measurements are included in Table 1.

From each of the observations we obtained an estimate of the magnitude difference Δm between the components of Wolf 424. Those measurements have been published by Henry et al. (1998). The average of the four determinations is $\Delta m = -0.01 \pm 0.02$, which formally indicates that the "secondary" is marginally brighter than the "primary" at this wavelength. The two stars are so similar that for all practical purposes the passband of these observations (F583W filter) is equivalent to V because the difference in the $B-V$ colors, which drives the conversion from ΔF583W to ΔV, is negligible (see Henry et al. 1999).

Another positional measurement with *HST* was recently published by Schultz et al. (1998), who observed Wolf 424 with the Faint Object Spectrograph used in imaging mode. We incorporate this observation into our analysis as well.

3. ORBITAL SOLUTION

As mentioned above, with observations of such diverse quality, the issue of the weighting in the least-squares solution becomes very important. Our approach here has been to set the weights w on the basis of the uncertainties directly estimated by the observers ($w = 1/\sigma^2$), to the extent that this is possible, with careful consideration of possible systematic errors. However, not always are the published uncertainties realistic nor do all observers publish uncertainties, so that some measure of personal judgment is unavoidable.

In Table 2 we list the uncertainties used initially for each source. The errors in the photographic observations are as published by Heintz (1972) for an observation of unit weight, converted from probable errors to mean errors, and expressed in polar coordinates. All normal places are weighted equally, since experiments with weights proportional to the plate weights published by Heintz (1972) indicated no improvement in the solutions discussed below. The visual observations are rarely given with errors, so we have tentatively adopted for all of them the same uncertainties as the photographic measurements because they seem to be of similar quality (see below). For the speckle measurements made by Balega et al. (1994) and Blazit et al. (1987), we adopted the uncertainties given by Henry et al. (1992), which we consider more reasonable.

An orbital solution including all available data was performed using standard nonlinear least-squares techniques (see, e.g., Press et al. 1992, p. 650), with all position angles precessed to the equinox 2000, and weights determined from Table 2. We minimized the quantity

$$\chi^2 = \sum \left(\frac{\theta - \theta_c}{\sigma_\theta}\right)^2 + \sum \left(\frac{\rho - \rho_c}{\sigma_\rho}\right)^2 + \sum \left(\frac{r - r_c}{\sigma_r}\right)^2, \quad (1)$$

where the three terms correspond to the position angles, the angular separations, and the one-dimensional speckle measurements by Henry et al. (1992) in the north-south direction, respectively. The symbols θ_c, ρ_c, and r_c represent the positions calculated from the orbital elements at each iteration.

This initial solution gave a period of 15.9 yr, a semimajor axis of 0.″89, and an eccentricity of 0.29. However, it also revealed significant patterns in the residuals of the visual and photographic observations indicating rather serious systematic errors, particularly in the angular separations. For example, the $O-C$ residuals in ρ for the photographic measurements came out predominantly negative, deviating from zero by more than 5 σ on average. Similarly, the visual

TABLE 2

UNCERTAINTIES FOR THE ASTROMETRIC OBSERVATIONS OF WOLF 424

References	Type	σ_θ	σ_ρ
1, 2, 3	Photographic[a]	0.048[b]	0.048[d]
3, 4, 5, 6, 7, 8, 9, 10, 11, 12, 13	Visual[a]	0.048[b]	0.048[d]
14	One-dimensional IR speckle	...	10[e]
14	Two-dimensional IR speckle	2[c]	4[e]
15	Two-dimensional visual speckle	2[c]	4[e]
16	Two-dimensional IR speckle	5[c]	5[e]
17	Two-dimensional IR speckle	5[c]	0.015[d]
18	Two-dimensional visual speckle	2[c]	4[e]
19	*HST*/FGS	0.0017[b]	0.0011[d]
20	*HST*/FOS	2.5[c]	0.027[d]

[a] Errors doubled in the final solution (see text).
[b] Units: arcsec ρ^{-1}.
[c] Units: degrees.
[d] Units: arcsec.
[e] Units: percent.

REFERENCES.—(1) Heintz 1972; (2) Luyten 1969; (3) Heintz 1989; (4) Reuyl 1938; (5) Kuiper 1938; (6) Worley & Douglass 1996; (7) Wilson 1954; (8) Worley 1962; (9) Worley 1972; (10) Couteau 1970; (11) van Biesbroeck 1975; (12) Heintz 1990; (13) Heintz 1993; (14) Henry et al. 1992; (15) Blazit et al. 1987; (16) Perrier et al. 1992; (17) Carbillet et al. 1996; (18) Balega et al. 1994; (19) this paper; (20) Schultz et al. 1998.

measurements of the angular separation showed an average residual exceeding 4 σ, also on the negative side. This is seen clearly in Figure 1*a*, in which we plot the visual and photographic residuals in ρ as a function of orbital phase. For the visual data (*circles*) we see no difference between observations made with small and with large telescopes, which suggests that the effect is essentially independent of aperture. The position angles, on the other hand, show no obvious bias (Fig. 1*b*), nor do we see any trend in the speckle or *HST* residuals.

That the photographic angular separations for Wolf 424 appear to be underestimated was already noted by Heintz (1972), who attempted to overcome this in his solution by allowing the visual observations to control the semimajor axis and leaving the photographic elongations on the small side. No speckle observations were available at the time. However, our solution indicates that the visual separations are significantly underestimated as well, and Schultz et al. (1998) reached the same conclusion.

For the photographic measures these systematic errors are understandable because of the difficulties of the plate technique in this particular case and its vulnerability to guiding and seeing conditions. The visual measurements are also very difficult because of the faintness of the components. Inclusion of these data with full weight in the least-squares solution would clearly bias the results, especially the semimajor axis upon which the total mass depends. Decreasing their weight, as done by Schultz et al. (1998), would alleviate the problem somewhat but the effect would still remain at a lower level. This is seen clearly by comparing their two solutions, one with the weights of the visual and photographic data reduced and the other using only speckle and *HST*/FOS measurements. Excluding the visual and photographic observations altogether is another possibility, but this would not take advantage of the long time coverage of those data, which extend back more than three orbital cycles from the first of the speckle observations. The position angles in particular yield valuable information about the period that we wish to retain here, especially since the modern measurements (speckle and *HST*) do not quite cover one orbital cycle. We have therefore chosen to exclude the photographic and visual separations but to keep the position angles, which show no serious systematic effects. However, we have increased the uncertainties of the position angles by a factor of 2 in view of the difficulties mentioned above.

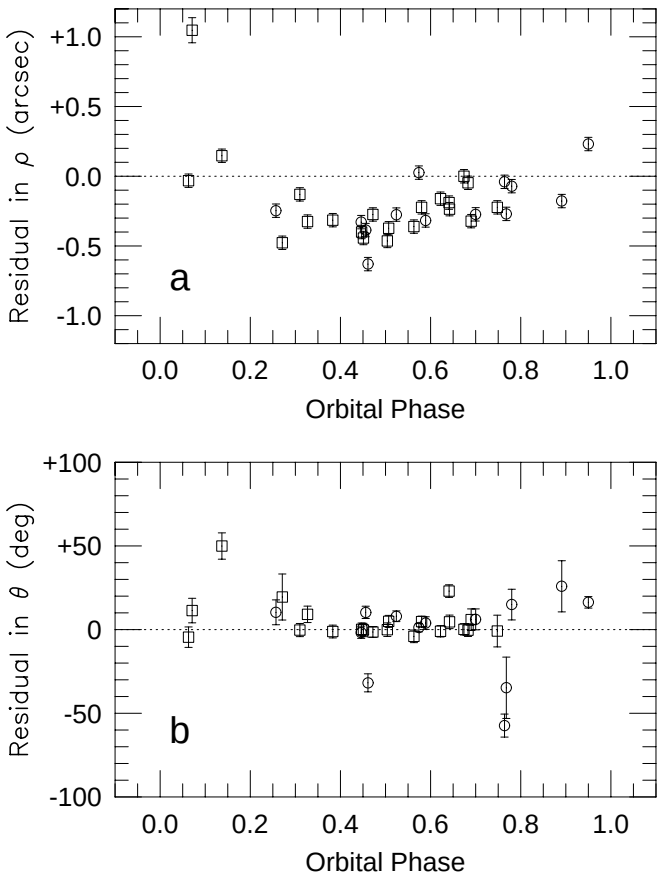

FIG. 1.—(*a*) $O-C$ residuals of the visual and photographic observations in angular separation as a function of orbital phase, from an orbital fit that includes all observations. Open circles are the visual observations, and open squares are photographic measurements. Systematic errors are evident in both kinds of observations. (*b*) Same as (*a*) for the position angles. No obvious biases are seen.

We then repeated the orbital solution using the visual and photographic position angles, the one-dimensional and two-dimensional speckle measurements, and the *HST* measurements. A few observations gave residuals larger than 3 σ and were rejected. These include two visual measurements (position angles) and two speckle measurements (separations). The elements we derive for the orbit are listed in Table 3, along with the solutions by Heintz (1989) and Schultz et al. (1998) (Orbit I) for comparison. The residuals of all observations are shown in Table 1, both in units of degrees and arcseconds (for θ and ρ) and also normalized by the corresponding errors (σ_θ and σ_ρ). The observations excluded from the fit have their residuals in parentheses in Table 1. We note that the standard deviation of the normalized visual and photographic position angle residuals is very close to unity, which suggests that the uncertainties we adopted for those measurements (twice the published estimates) are realistic. Although these position angles show no strong systematic deviations (see Fig. 1*b*) at the level displayed by the visual and photographic angular separations, we do notice that the θ residuals are all negative up to 1955 and mostly positive thereafter. Nevertheless, they are still well within our 3 σ rejection limit. A hint of the same trend is seen in Heintz's (1972) (pre-speckle) residuals and to some extent also in the solution by Schultz et al. (1998).

The orbit is displayed graphically in Figure 2 together with the two-dimensional speckle and *HST* observations, which are the only ones that contain useful information on the angular separation and can be displayed in polar coordinates. We show also for comparison the orbits by Heintz (1989) and Schultz et al. (1998). Neither of these two solutions fits the *HST* observations or some of the speckle measurements very well. The information on the position angles contributed by the visual and photographic observations is shown in Figure 3*a*, in the form of a diagram of θ versus orbital phase. We include the other two-dimensional measurements for completeness. The one-dimensinal speckle observations in the north-south direction reported by Henry et al. (1992) are the earliest speckle observations available that contain useful information on the angular separation of Wolf 424. In Figure 3*b* we compare these one-dimensional observations and also the north-south separations for the two-dimensional measurements against the north-south separations predicted by our orbital solu-

TABLE 3

ORBITAL SOLUTIONS FOR WOLF 424

Element	Heintz (1989)[a]	Schultz et al. (1998)	This Paper
P (yr)	16.2	15.2 ± 0.1	15.643 ± 0.096
a (arcsec)	0.715 ± 0.04	0.747 ± 0.02	0.9257 ± 0.0049
a (AU)	3.07[b]	3.21 ± 0.14[b,c]	4.062 ± 0.098
e	0.28	0.27 ± 0.01	0.2950 ± 0.0035
i (deg)	103	105.0 ± 1.3	103.00 ± 0.15
ω_B (deg)	20	3.79 ± 8.0	347.2 ± 1.5
Ω_{2000} (deg)	151	142.26 ± 1.9	143.48 ± 0.19
T	1993.8[d]	1992.9 ± 0.7[d]	1992.297 ± 0.056
$M_A + M_B$ ($M_\odot$)	0.110	0.143 ± 0.012[b]	0.274 ± 0.020[e]
M_A ($M_\odot$)	0.059	0.076 ± 0.007[b,c]	0.143 ± 0.011[e,f]
M_B ($M_\odot$)	0.051	0.067 ± 0.006[b,c]	0.131 ± 0.010[e,f]
N_θ	29	25	50
N_ρ	29	25	14
$N_{1\text{-D}}$	0	0	4
Time span (yr)	53.0	57.9	59.9

[a] In a subsequent paper (Heintz 1993) a slightly shorter orbital period of 16.0 yr was proposed.
[b] Adopted parallax in original paper is $\pi_{trig} = 0''.233 \pm 0''.004$.
[c] Uncertainty added here.
[d] Shifted by an integer number of cycles for comparison purposes.
[e] Adopted parallax is $\pi_{trig} = 0''.2279 \pm 0''.0046$.
[f] Adopted mass fraction is $f = 0.477 \pm 0.008$.

tion. Inclusion of the one-dimensional speckle points allows us to nearly close the orbit with data from modern techniques.

Our orbital solution represents the best fit to all available data that show no significant systematic errors. Although the visual and photographic measurements make some contribution to the period and other elements, the scale of the orbit is set entirely by the speckle and *HST* observations. A solution with just the modern data (speckle + *HST*) gives nearly the same orbital elements. Similarly, using only the

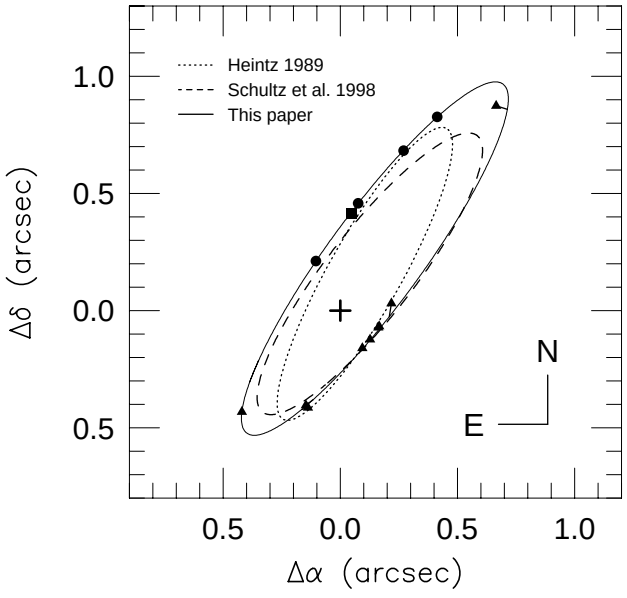

FIG. 2.—Orbital solution for Wolf 424 (*solid line*) together with all two-dimensional speckle measurements (*triangles*) and *HST* observations. Filled circles represent our own *HST*/FGS measurements, and the square is for the Schultz et al. (1998) *HST*/FOS observation. Residual vectors are plotted with thin lines but are typically smaller than the symbol size. Also shown for comparison are the orbits obtained by Heintz (1989) (*dotted line*) and Schultz et al. (*dashed line*).

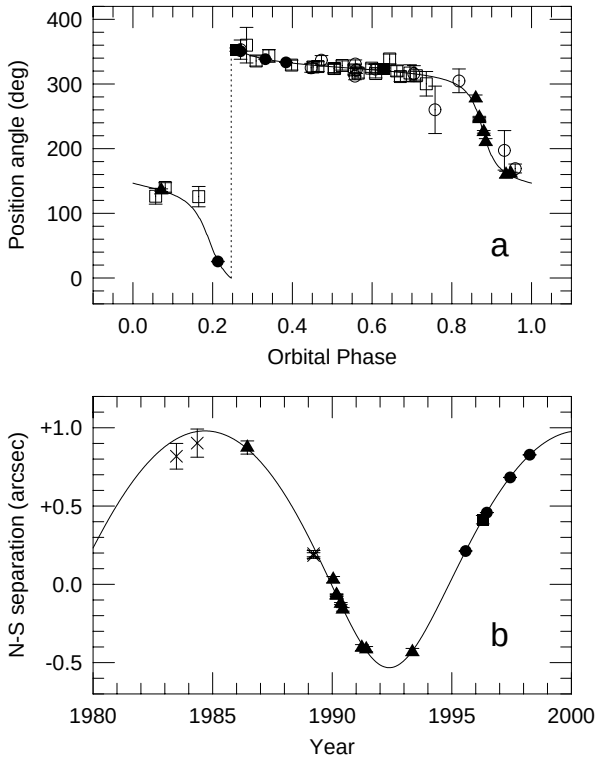

FIG. 3.—(*a*) Position angles as a function of orbital phase for the visual and photographic observations, which are not displayed in Fig. 2. For completeness we show also the speckle and *HST* measurements. Symbols are as in Figs. 1 and 2. (*b*) Angular separations for Wolf 424 projected in the north-south direction to illustrate the orbital fit to the one-dimensional speckle measurements by Henry et al. (1992) (*crosses*). The error bars for many of the observations are too small to be seen on this figure.

one-dimensional and two-dimensional speckle measurements and excluding the *HST* data also gives similar orbital elements. In particular, the semimajor axis and therefore the total mass is the same in all cases, within the errors.

4. INDIVIDUAL MASSES

From the elements listed in Table 3 and the known trigonometric parallax of the system ($\pi_{\rm trig} = 0\farcs2279 \pm 0\farcs0046$; van Altena et al. 1995), the total mass for Wolf 424 is $M_{\rm tot} = 0.274 \pm 0.020\ M_\odot$. The precision of the total mass (7%) is limited mostly by the parallax error, which contributes nearly $\frac{3}{4}$ to the total uncertainty. This is clearly one area in which there is room for significant improvement. The dynamical quantity a^3/P^2 is determined to considerably better precision (<2%): 0.003242 ± 0.000058 arcsec^3 yr^{-2}.

In addition to the total mass of a visual binary, knowledge of either the mass ratio ($q = M_{\rm B}/M_{\rm A}$) or the mass fraction [$f = M_{\rm B}/(M_{\rm A} + M_{\rm B})$] is required in order to determine individual masses dynamically. Unfortunately, no radial velocity information is available for the components of Wolf 424 separately, which would yield a direct measure of q. However, perturbations in the motion of a photographically unresolved system such as Wolf 424 revealed by plates taken over several decades provide useful information on the mass fraction of the binary. The photographic measurements are assumed to refer to the center of light of the system, which moves around the center of mass. Once the system is resolved by other techniques and the *relative* motion becomes known, as is the case here, the mass fraction may be determined from $f = (\alpha/a) + \beta$, where α is the semimajor axis of the photocentric orbit (measured photographically), and a is the semimajor axis of the relative orbit (see, e.g., van de Kamp 1967, p. 141). The quantity $\beta = l_{\rm B}/(l_{\rm A} + l_{\rm B})$ is the fractional luminosity and also represents the fractional distance of the primary to the photocenter in terms of the separation between the two components. For small magnitude differences (Δm), β is given directly as $\beta = (1 + 10^{0.4\Delta m})^{-1}$.

Few independent estimates of semimajor axis of the photocentric orbit of Wolf 424 have been published. Upgren & Mesrobian (1971) reported that the residuals from the plate solutions for parallax and proper motion at the Van Vleck Observatory indicated a peak-to-peak amplitude of the displacement of the photocenter of about 0.″032 in the x coordinate (R.A.), and a smaller (unspecified) amplitude in y (decl.). From this we infer a semiamplitude of at least $\alpha = -0\farcs016$. The negative sign we have added simply reflects the convention that α is taken to be positive when the photocenter and the secondary are on opposite sides of the barycenter.

An independent estimate of the photocentric semimajor axis from the Sproul plate material was published by Heintz (1972), who obtained $\alpha = -0\farcs007 \pm 0\farcs005$. Heintz then used his relative semimajor axis ($a = 0\farcs76$) and a magnitude difference of $\Delta m = 0.0$ to derive $f = 0.49 \pm 0.01$. Additional plate measurements at Sproul led to a revised estimate of α, published only in the form of the photocentric factor $f - \beta = -0\farcs033 \pm 0\farcs008$ (Heintz 1989). Since this implicitly makes use of Heintz's revised semimajor axis ($a = 0\farcs715 \pm 0\farcs04$), and since the value of a we derive here is somewhat different (see Table 3), we first reconstructed α using Heintz's value of a, obtaining $\alpha = -0\farcs0236 \pm 0\farcs0059$.

The mass fraction then follows from our own determination of a and our magnitude difference provided by the new *HST*/FGS measurements. As mentioned earlier, these measurements are in a passband near V, which is sufficiently close for our purposes to the effective wavelength of the photographic observations. The average magnitude difference from our four *HST*/FGS measurements is $\Delta m = -0.01 \pm 0.02$. We then find $\beta = 0.502 \pm 0.005$ and derive the mass fraction $f = 0.477 \pm 0.008$, which is close to Heintz's most recent determination ($f = 0.467 \pm 0.01$; Heintz 1990). Finally, the mass fraction and total mass lead to individual masses for Wolf 424A and B of $M_{\rm A} = 0.143 \pm 0.011\ M_\odot$ and $M_{\rm B} = 0.131 \pm 0.010\ M_\odot$, respectively. The relative errors are approximately 8%.

5. LUMINOSITIES AND COLORS

The difference in brightness between the components of Wolf 424 has been measured on several occasions in different passbands. Henry et al. (1992) obtained magnitude differences at J, H, and K from their speckle observations. Another estimate in the K band was published by Perrier et al. (1992). At shorter wavelengths the brightness difference is known to be small. Our own measurements with *HST*/FGS indicate a mean consistent with zero. Schultz et al. (1998) gave an estimate also close to zero from their observation with *HST*/FOS, which has a bandpass approximately B. We have taken the average of all measurements in each filter and have collected the results in the first column of Table 4.

The trend of these average magnitude differences is not at all what one would expect for normal stars in a binary, where the secondary should become comparatively brighter (smaller Δm) toward longer wavelengths. In Wolf 424 the brightness difference *increases* redward. This suggests perhaps some color anomaly in one or both stars.

Photometric measurements of the combined light of the binary have been made by a number of authors over a broad wavelength range, from the U band (0.36 μm) to the M band (5 μm). It has also been detected by the IRAS satellite at 12 μm. In Table 4 we present the averages of independent measurements from the literature in the bands in which the magnitude difference between the stars has also been determined (B, V, J, H, K). From these we have inferred the brightness of each component separately to examine their photometric properties more closely.

We first compare the observed colors of Wolf 424A and B to those of normal M dwarfs, as represented by the empirical relations derived by Henry & McCarthy (1993). These are published in the form of polynomial fits to the $V - x$ indices as a function of the absolute magnitudes M_x, where x is J, H, or K. We have added to these fits a similar relation for $B-V$ versus M_B, derived here from the nearby sample used by Henry & McCarthy and using similar sources for the photometry (Leggett 1992; Weis 1996). In addition, we make use of the known parallax of the system to compute M_x.

The comparison is shown in Figure 4 in the form of differences between the measured $V - x$ indices and those derived from the empirical relations. The error bars include the contributions from the uncertainties in the observed magnitude differences, the combined magnitudes, and in the trigonometric parallax. This purely photometric test reveals that component B has more or less normal colors. The primary component, on the other hand, shows a marked

TABLE 4

MAGNITUDE DIFFERENCES, COMBINED MAGNITUDES, AND INDIVIDUAL APPARENT MAGNITUDES FOR THE COMPONENTS OF WOLF 424

Passband	Δm	$N_{\Delta m}$	References	Combined Magnitude	N_{tot}	References	Component A	Component B
B (0.45 μm)	0.05	1	1	14.31 ± 0.02	29	5, 6, 7, 8, 9, 10	15.04 ± 0.03	15.09 ± 0.03
V (0.55 μm).....	-0.01 ± 0.02	4	2	12.46 ± 0.01	63	5, 6, 7, 8, 9, 10, 11, 12	13.22 ± 0.01	13.21 ± 0.01
J (1.25 μm)	0.13 ± 0.04	2	3	6.99 ± 0.02	8	6, 9, 13, 14, 15	7.68 ± 0.03	7.81 ± 0.03
H (1.65 μm).....	0.20 ± 0.07	3	3	6.39 ± 0.01	8	6, 9, 13, 14, 15	7.05 ± 0.03	7.25 ± 0.04
K (2.20 μm).....	0.44 ± 0.09	6	3, 4	6.04 ± 0.02	8	6, 9, 13, 14, 15	6.60 ± 0.04	7.04 ± 0.06

REFERENCES.—(1) Schultz et al. 1998; (2) Henry et al. 1998; (3) Henry et al. 1992; (4) Perrier et al. 1992; (5) Rucinski 1981; (6) Stauffer & Hartmann 1986; (7) Sandage & Kowal 1986; (8) Bessell 1990; (9) Doyle & Butler 1990; (10) Landolt 1992; (11) Kunkel & Rydgren 1979; (12) Weis 1994; (13) Glass 1975; (14) Probst 1981; (15) Simons, Henry, & Kirkpatrick 1996.

departure from mean colors of similar stars, and the discrepancy increases toward longer wavelengths. Wolf 424A appears too red by almost a magnitude at $V-K$, but without further information we cannot distinguish from this diagram alone whether this is caused by infrared excess, or whether the star is too faint at the shorter wavelengths for some reason.

Further insight may be gained by using the mass information provided by our orbital solution and the empirical MLRs by Henry & McCarthy (1993). These relations allow us to predict the absolute magnitudes at various wavelengths for a given mass, which is in essence a check on the spectral energy distribution (SED) of each component. To complement the MLRs by Henry et al. at V, J, H, and K, we have constructed one at B using their fit in the V band together with the $B-V$ versus M_B relation derived above.

If we use the individual masses as obtained in § 4 we find that the predicted absolute magnitudes for both stars are too bright by several tenths of a magnitude and by more than a magnitude at B and V for the primary, much beyond the observational errors (see Fig. 5, *open circles*). There are several possible reasons for this, including errors in our orbital solution (a^3/P^2), in the adopted mass fraction f, or differences in age and/or metallicity between Wolf 424 and the average star represented by the MLRs (cosmic scatter). The cosmic scatter can amount to 0.3–0.5 mag (see Henry & McCarthy 1993), which is about the difference found for the secondary. We cannot rule out some contribution of this nature, but it seems unlikely it could account for the full offset in B and V for the primary. Another explanation could be errors in the parallax, which affect not only our masses but also the absolute magnitudes. The uncertainty

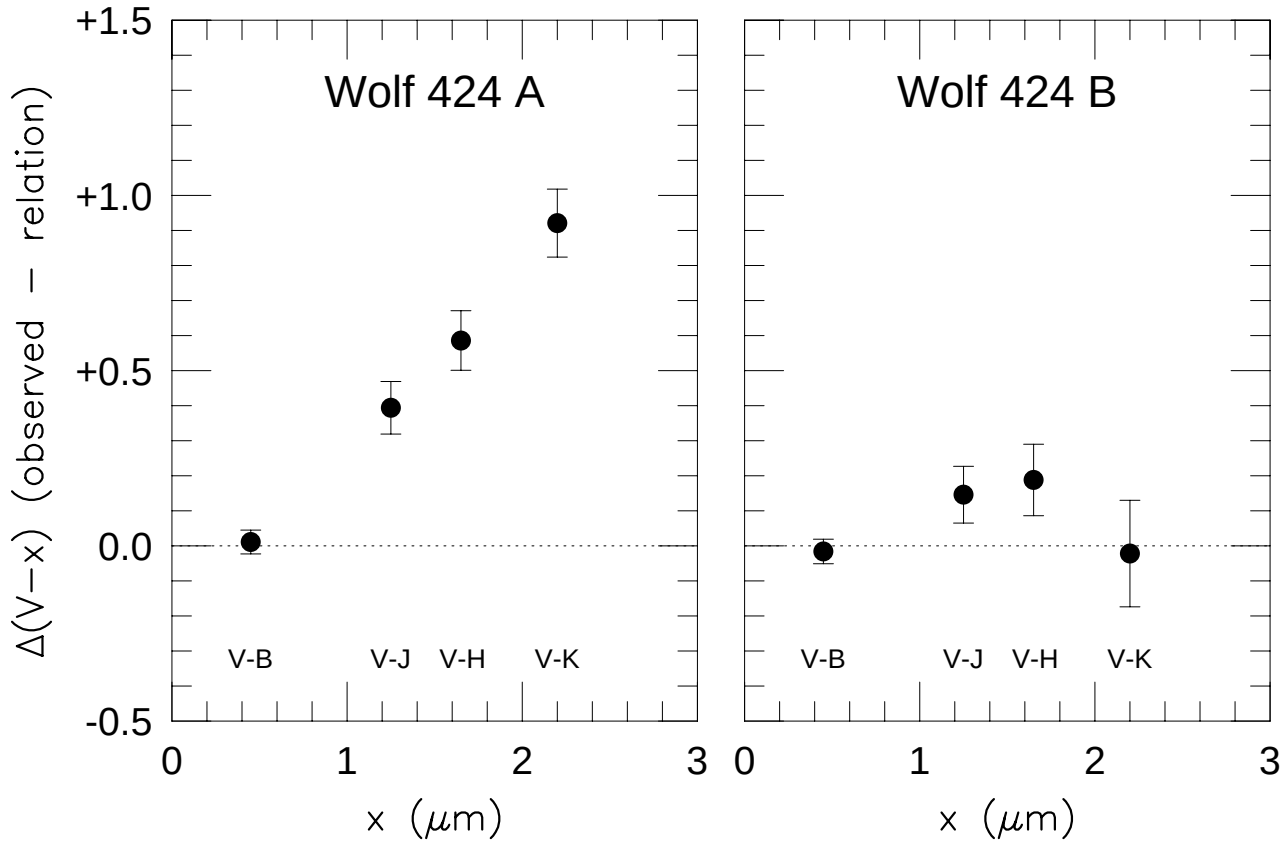

FIG. 4.—Difference between the observed color indices of Wolf 424A and B and the colors predicted using the relations by Henry & McCarthy (1993). While the secondary behaves roughly as expected, the primary shows significant differences compared to a "normal" M dwarf.

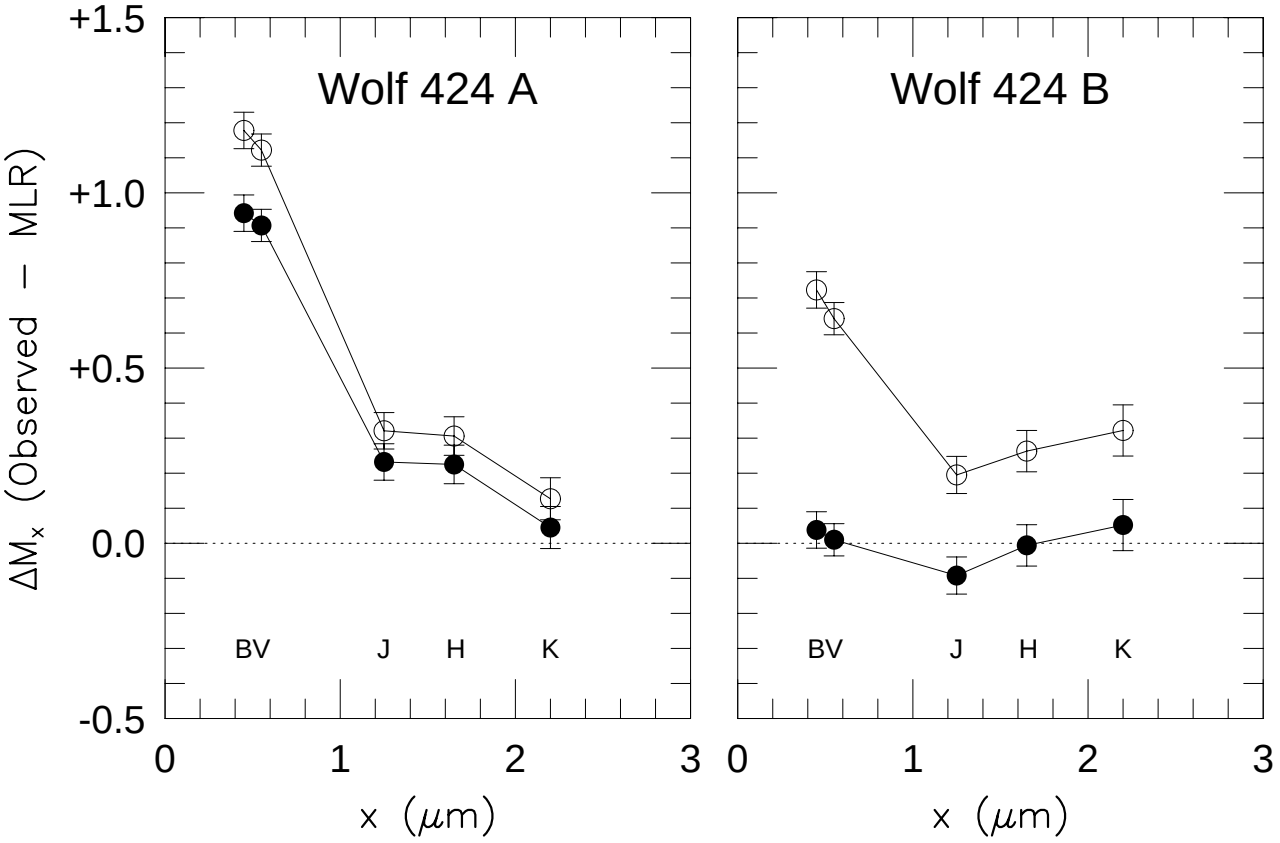

FIG. 5.—Difference between the observed absolute magnitudes of Wolf 424A and B and the brightness predicted using the empirical MLRs by Henry & McCarthy (1993). Open symbols represent the differences obtained by using the measured values of the parallax ($\pi_{trig} = 0''.2279$) and mass fraction ($f = 0.477$). Filled symbols show the result when adjusting those quantities slightly ($\pi_{trig} = 0''.235, f = 0.457$) to minimize the differences for the secondary (see text). The primary is seen to be increasingly too faint toward the shorter wavelengths compared to a "normal" M dwarf.

in the parallax is in fact the main contributor to the errors in the other derived quantities.

Since the colors of component B appear to be normal (Fig. 4), we experimented with small changes in the parallax and mass fraction to see if an adjustment could produce predicted absolute magnitudes for that star also in agreement with the observations. We first tried varying π_{trig} and f independently and found that the corrections required in each case were quite significant in terms of the quoted uncertainties in those quantities, as large as 7 σ in the case of f. Adjusting both quantities simultaneously also allowed us to obtain good agreement between the empirical MLRs and the observations for the secondary, for $\pi_{trig} = 0''.235$ and $f = 0.457$, which are only about 1.5 σ and 2.5 σ different from the measured values.[3] The corresponding masses for the two stars are $M_A = 0.137\ M_\odot$ and $M_B = 0.116\ M_\odot$, which are also not far from the values derived in § 4. Figure 5 (*filled circles*) shows the magnitude differences we obtain for Wolf 424A and B using these values, in the sense ⟨observed − empirical MLR⟩.

These experiments show that, through slight adjustments in the parallax and the mass fraction, not only can the predicted SED for the secondary be made consistent with the observations but also that the K magnitude of the primary is in agreement with the empirical relations. Therefore, it is the brightness at shorter wavelengths that is different in this star. We elaborate on possible causes in the next section.

A small adjustment in the parallax, as found above, will change Figure 4 slightly, but not the conclusion we derive from it regarding the anomalous colors of the primary.

6. DISCUSSION

The orbital solution presented in § 3 and Figure 2, in which the scale is set by modern measurements of the angular separation with *HST* and the speckle technique, leaves little doubt that the masses of Wolf 424A and B are well above the substellar limit. Although the systematic errors in the visual and photographic angular separations have been recognized before, the inclusion of those observations in previous analyses (even with reduced weight) has consistently resulted in a smaller semimajor axis and consequently in masses that appeared to lie in the brown dwarf regime. It seems clear in light of the new measurements (particularly our high-precision *HST*/FGS observations) that the difficult visual and photographic separations should not be used in the solution.

Despite this bias, the duplicity of the system is clearly detected in those observations, and the changes in ρ can be followed roughly. In fact, previous orbital analyses for Wolf

[3] The published parallax for Wolf 424 (van Altena et al. 1995) is the weighted average of seven measurements that do not always agree within their quoted errors. It is interesting to note that if the two most discrepant values are removed, the weighted parallax becomes $\pi_{trig} = 0''.234$, nearly identical to our result here.

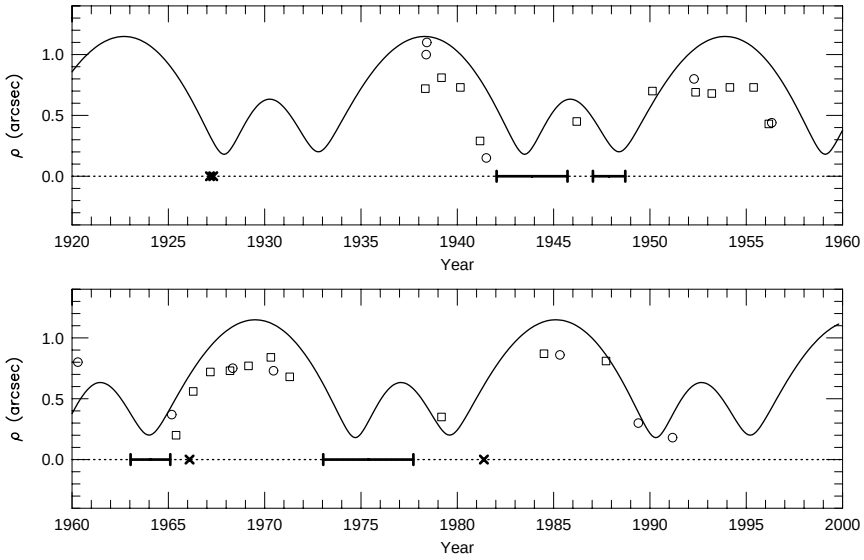

FIG. 6.—Predicted angular separation as a function of time from our orbital solution. The crosses and intervals indicated along the dotted line represent the times at which Wolf 424 was reported to be unresolved on photographic plates. Resolved observations are also shown (open circles for visual measurements and open squares for photographic measurements).

424 have been influenced to some degree by the need to reproduce the absence of elongation in the photographic images in certain years (Heintz 1972; Schultz et al. 1998). Without having imposed this requirement explicitly here, our solution does remarkably well in this regard, as shown in Figure 6. All instances reported in the literature in which the system was unresolved (*round images on the plates*) are seen to fall at or near a minimum in the predicted angular separation.

The individual masses we obtain have formal errors just under 8% and are thus among the most precisely determined for low-mass stars. They are currently limited mostly by the error in the (ground-based) parallax. The *Hipparcos* satellite did not observe Wolf 424, but it is likely that the duplicity of the object would have compromised the accuracy of the trigonometric parallax in any case, especially given the small angular separation at the time of the space mission. In the absence of radial velocity information, we have split the total mass into separate components using the mass fraction determined astrometrically, which hinges on the semimajor axis of the photocentric orbit derived from photographic plates. Complete details on the determinations of α have not been published, and we have accepted this quantity more or less at face value. The two available estimates of α ($-0\farcs007 \pm 0\farcs005$, Heintz 1972; and $-0\farcs0236 \pm 0\farcs0059$, Heintz 1989; see § 4), which are not completely independent, differ by slightly more than twice their internal errors, however, so it is possible that the uncertainty we have adopted here for f is somewhat underestimated.

Wolf 424 is among the handful of systems with reliable individual masses below 0.2 $M_\odot$ determined dynamically. In Figure 7 we show the location of the components in the K-band mass-luminosity diagram. The photometry and masses for the other stars shown are taken from the work of Henry & McCarthy (1993) and Henry et al. (1999). This figure represents an update of the diagram presented by Henry et al. (1992), which showed Wolf 424A and B deviating considerably from the trend defined by other low-mass dwarfs because of the lower masses they were thought to have. With the masses we derive here, the apparent discrepancy is resolved: the components are clearly *not* brown dwarfs. The dotted line in the figure represents the fit by Henry & McCarthy (1993), which is still a very good representation of the empirical M-L relation.

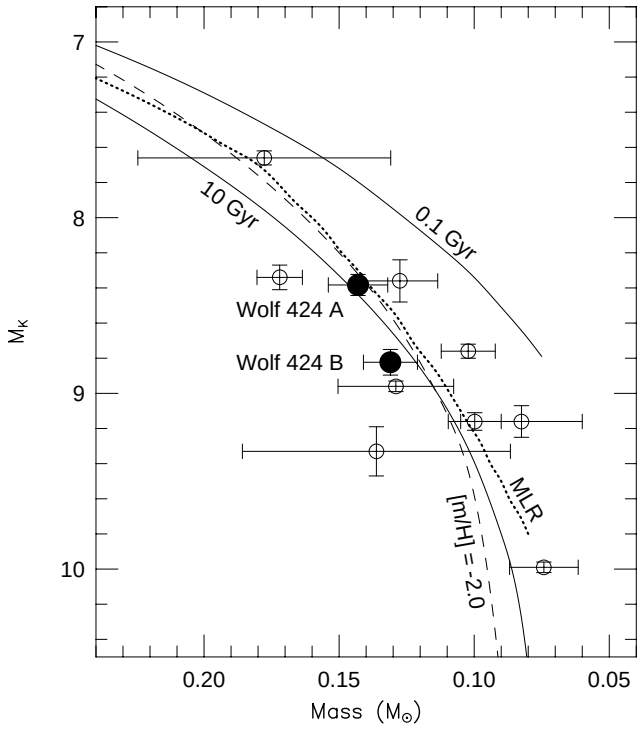

FIG. 7.—Mass-luminosity relation in the K band for low-mass stars (see text). Wolf 424A and B are represented by the filled circles. The dotted line represents the empirical fit by Henry & McCarthy (1993); the solid lines are from theoretical models by Baraffe et al. (1998) for solar metallicity and ages of 10 Gyr and 0.1 Gyr. Also shown is an isochrone for 10 Gyr and $[m/\mathrm{H}] = -2.0$ (*dashed line*) from models by Baraffe et al. (1997), to illustrate the effect of metallicity.

Theoretical evolutionary models for low-mass stars have advanced considerably in recent years (Chabrier, Baraffe, & Plez 1996; Baraffe et al. 1997, 1998). To illustrate the fit between recent models and the observations at the low-mass end of the MLR, we show in Figure 7 two isochrones by Baraffe et al. (1998) for solar metallicity and ages of 10 Gyr and 0.1 Gyr (*solid lines*). The 10 Gyr curve is consistent with our determinations for Wolf 424. Metal abundance has a relatively small effect in this mass range, as illustrated in the figure by a 10 Gyr isochrone with $[m/\mathrm{H}] = -2.0$ (Baraffe et al. 1997), indicated by the dashed line.

The photometric anomalies detected in Wolf 424A may preclude the primary from being used in future empirical fits of *optical* MLRs, such as that of Henry et al. (1999). The V magnitude of that star appears to be roughly 1.0 mag too faint compared to normal M dwarfs (Fig. 5). A plausible explanation for this is the presence of surface features (spots), which are known to affect the luminosity of a star at optical wavelengths but are much less noticeable toward the infrared. Indeed, Figure 5 indicates essentially no effect in the K band. Given the large effect observed in V, it would appear that the spot coverage is quite significant. Wolf 424 is a very active flare star, with an estimated flare rate in the optical of about five events per hour (Moffet 1973; Gershberg & Shakhovskaya 1983; Beskin et al. 1988). Spottedness is a common phenomenon in active M dwarfs, directly related to the flares and other manifestations of chromospheric activity. The observed photometric properties of the primary in this system are therefore not at all surprising. They may even suggest that the primary is in fact largely responsible for the flaring activity. Some support for this was presented by White, Jackson, & Kundu (1989), who reported the detection of radio emission from Wolf 424 in a survey of nearby flare stars with the VLA, but only from one component, which they concluded was the primary.

In addition to the observed rapid changes in brightness from flaring (mainly in U and B), one might expect also photometric variability on longer timescales related to the spot coverage such as rotational modulation or intrinsic changes in the spot properties, and even magnetic activity cycles. Photoelectric monitoring in the V, R, and I bands by Weis (1994) revealed no significant changes greater than 0.007 mag in Wolf 424 over a period of 9 yr. Another study by Bondar' (1995) was based on photographic plates from the archives of the Sternberg State Astronomical Institute (Russia) and the Sonneberg Observatory (Germany) covering several decades. These measurements clearly reveal what appear to be periodic changes in the brightness of the system, with a total amplitude of about 0.2 mag (see Fig. 8*a*). We have subjected the original data, kindly provided by N. Bondar', to a power spectrum analysis using the CLEAN algorithm (Roberts, Lehar, & Dreher 1987). The period we obtain is 15.8 yr (Fig. 8*c*). Although it is tempting to ascribe this variation to the magnetic activity cycle (a complicated interpretation given the binary nature of the object), we note that the period is suspiciously close to the orbital period of Wolf 424 (15.6 yr). Furthermore, a comparison of Figure 8*a* and Figure 6 shows that the maximum brightness as measured photographically coincides in time with the maximum angular separation and similarly with the minima. Because the estimates of the photographic magnitudes were made visually, it appears likely that those measurements actually refer to the size of the elongated images, which obviously correlates with orbital motion.

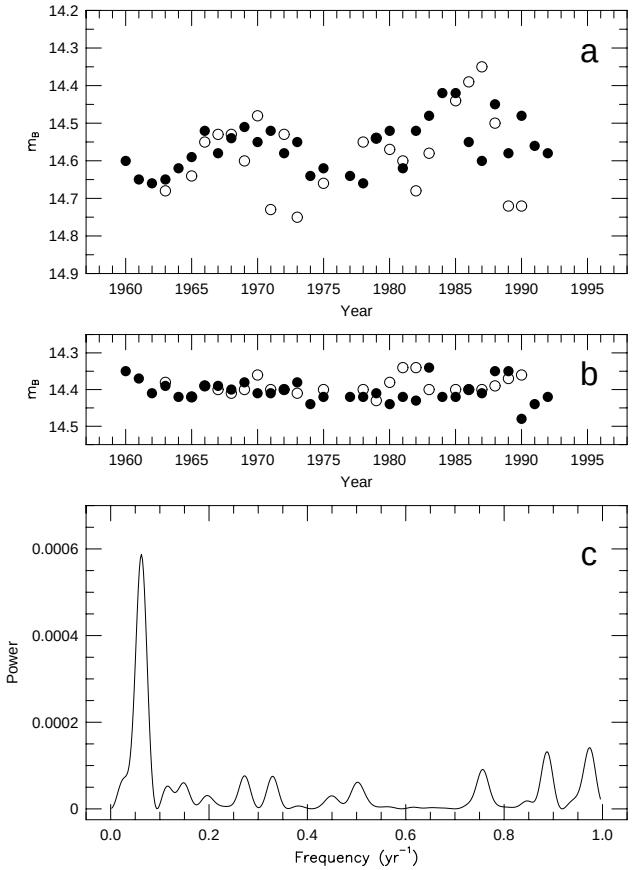

FIG. 8.—(*a*) Photographic magnitude of Wolf 424AB over the past three decades as measured by Bondar' (1995). Measurements are based on plates from the archives of the Sternberg State Astronomical Institute (*filled circles*) and the Sonneberg Observatory (*open circles*). (*b*) Comparison star on the same vertical scale. (*c*) Power spectrum of the data in (*a*) computed with the CLEAN algorithm (Roberts et al. 1987) showing a peak corresponding to a period of 15.8 yr.

Thus we believe that these apparent changes in brightness are simply a reflection of the ~ 16 yr orbit of Wolf 424.

7. CONCLUSIONS

We have obtained new *HST*/FGS measurements of Wolf 424 over a period of 3 yr that strongly constrain the astrometric orbit of this late-type binary. Previous analyses have relied to some extent on the visual and photographic observations of the system, which are seriously biased in angular separation (but not in position angle). Our new orbital solution makes use of all available positional information that is free from any significant systematic errors.

With the known parallax and mass fraction and our new orbital solution, the masses we derive ($M_A = 0.143 \pm 0.011$ $M_\odot$ and $M_B = 0.131 \pm 0.010$ $M_\odot$) place both components clearly above the substellar limit. The orbit is sufficiently well covered now that further measurements in coming years are unlikely to change these values significantly. These determinations are among the most precise for such low-mass stars and are thus important for establishing the empirical mass-luminosity relation near the end of the main sequence. Further improvement in the precision of these masses must come from a better determination of the parallax, which is currently contributing most of the error.

Roughly a dozen nearby M dwarfs under 0.2 $M_\odot$ now have their masses determined dynamically to moderately

good precision (Henry et al. 1999). These determinations are becoming increasingly important to test models of stellar evolution for low-mass stars, a very active area of research in recent years. The example of Wolf 424 shows that there is good agreement in the M-L plane with the latest generation of models by Baraffe et al. (1998) that incorporate updated interior physics and realistic boundary conditions set by nongray model atmospheres. The mass determinations at the low end of the main sequence will provide even stronger constraints on theory when accurate metallicity determinations for late-type M dwarfs become available, another area in which great progress is being made (see, e.g., Jones et al. 1996; Viti et al. 1997; Leggett, Allard, & Hauschildt 1998).

The differential photometry (from speckle observations and our new *HST*/FGS measurements) available for Wolf 424 and measurements of the combined light of the system in several passbands have revealed that the primary component is fainter than normal toward shorter wavelengths when compared to the average M dwarf with a similar mass. Spottedness is a likely explanation, consistent with the level of activity that is characteristic of flare stars such as Wolf 424.

We are grateful to N. I. Bondar' for providing her original measurements of the photographic magnitude of Wolf 424. We also thank the referee for helpful comments. Support for this work was provided by NASA through grants GO-06047.03-94A, GO-06566.03-95A, and GO-07493.01-96A from the Space Telescope Science Institute, which is operated by the Association of Universities for Research in Astronomy, Incorporated, under NASA contract NAS 5-26555. T. J. H. received additional support from NASA through Hubble Fellowship grant HF-1058.01-94A, also from STScI. Members and associates of the Space Telescope Astrometry Team received additional support from NASA under grant NAG5-1603 awarded to the University of Texas. This research has made use of the SIMBAD database, operated at CDS, Strasbourg, France.

REFERENCES

Allard, F., Hauschildt, P. H., Alexander, D. R., & Starrfield, S. 1997, ARA&A, 35, 137
Balega, I. I., Balega, Y. Y., Belkin, I. N., Maximov, A. F., Orlov, V. G., Pluzhnik, E. A., Shkhagosheva, Z. U., & Vasyuk, V. A. 1994, A&AS, 105, 503
Baraffe, I., Chabrier, G., Allard, F., & Hauschildt, P. H. 1997, A&A, 327, 1054
———. 1998, A&A, 337, 403
Beskin, G., Gershberg, R. E., Neizvestnyj, S. I., Plakhotnichenko, V. L., Pustil'nik, L. A., & Shvartsman, V. P. 1988, Izv. Krymskoi. Astrofiz. Obs., 79, 71
Bessell, M. S. 1990, A&AS, 83, 357
Blazit, A., Bonneau, D., & Foy, R. 1987, A&AS, 71, 57
Bondar', N. I. 1995, A&AS, 111, 259
Burrows, A., et al. 1997, ApJ, 491, 856
Carbillet, M., Ricort, G., Aime, C., & Perrier, Ch. 1996, A&A, 310, 508
Chabrier, G., Baraffe, I., & Plez, B. 1996, A&A, 459, 91
Couteau, P. 1970, A&AS, 3, 51
Davidge, T. J., & Boeshaar, P. C. 1991, AJ, 107, 267
Doyle, J. G., & Butler, C. J. 1990, A&A, 235, 335
Franz, O. G., Wasserman, L. H., Nelan, E., Lattanzi, M. G., Bucciarelli, B., & Taff, L. G. 1992, AJ, 103, 190
Gershberg, R. E., & Shakhovskaya, N. I. 1983, Ap&SS, 95, 235
Glass, I. S. 1975, MNRAS, 171, 19P
Heintz, W. D. 1972, AJ, 77, 160
———. 1989, A&A, 217, 145
———. 1990, AJ, 99, 420
———. 1993, A&A, 277, 452
———. 1994, AJ, 108, 2338
Henry, T. J., Franz, O. G., Wasserman, L. H., Benedict, G. F., Shelus, P. J., Ianna, P. A., Kirckpatrick, J. D., & McCarthy, D. W., Jr. 1999, ApJ, in press
Henry, T. J., Johnson, D. S., McCarthy, D. W., & Kirkpatrick, J. D. 1992, A&A, 254, 116
Henry, T. J., & McCarthy, D. W., Jr. 1993, AJ, 106, 773
Jones, H. R. A., Longmore, A. J., Allard, F., & Hauschildt, P. H. 1996, MNRAS, 280, 77
Kuiper, G. P. 1938, ApJ, 88, 472
Kunkel, W. E., & Rydgren, A. E. 1979, AJ, 84, 633
Landolt, A. U. 1992, AJ, 104, 340
Leggett, S. K. 1992, ApJS, 82, 351
Leggett, S. K., Allard, F., & Hauschildt, P. H. 1998, ApJ, 509, 836
Luyten, W. J. 1969, Univ. Minnesota Palomar Survey, No. 21
Magazzù, A., Martín, E. L., & Rebolo, R. 1993, ApJ, 404, L17
Marley, M. S., Saumon, D., Guillot, T., Freedman, R. S., Hubbard, W. B., Burrows, A., & Lunine, J. I. 1996, Science, 272, 1919
Moffet, T. J. 1973, MNRAS, 164, 11
Perrier, Ch., Mariotti, J.-M., Bonneau, D., & Duquennoy, A. 1992, in High-Resolution Imaging by Interferometry II. Ground-Based Interferometry at Visible and Infrared Wavelengths. Part I. Single Aperture Interferometry (ESO Conf. Proc. 39), ed. J. M. Beckers & F. Merkle (Garching: ESO), 109
Press, W. H., Teukolsky, S. A., Vetterling, W. T., & Flannery, B. P. 1992, Numerical Recipes (2d ed.; Cambridge: Cambridge Univ. Press)
Probst, R. G. 1981, Ph.D. thesis, Univ. of Virginia, Charlottesville
Reuyl, D. 1938, Harvard Announcement Card No. 449
———. 1941, PASP, 53, 336
Roberts, D. H., Lehar, J., & Dreher, J. W. 1987, AJ, 93, 968
Rucinski, S. M. 1981, Acta Astron., 31, 363
Sandage, A., & Kowal, C. 1986, AJ, 91, 1140
Saumon, D., Chabrier, G., & van Horn, H. M. 1995, ApJS, 99, 713
Schultz, A. B., et al. 1998, PASP, 110, 31
Simons, D. A., Henry, T. J., & Kirkpatrick, J. D. 1996, AJ, 112, 2238
Stauffer, J. R., & Hartmann, L. W. 1986, ApJS, 61, 531
Upgren, A. R., & Mesrobian, W. S. 1971, AJ, 76, 78
van Altena, Lee, J. T., & W. F., Hoffleit, E. D. 1995, The General Catalogue of Trigonometric Parallaxes (4th ed.; New Haven: Yale Univ. Obs.)
van Biesbroeck, G. 1975, ApJS, 28, 413
van de Kamp, P. 1967, Principles of Astrometry (San Francisco: W. H. Freeman)
Viti, S., Jones, H. R. A., Schweitzer, A., Allard, F., Hauschildt, P. H., Tennyson, J., Miller, S., & Longmore, A. J. 1997, MNRAS, 291, 780
Weis, E. W. 1994, AJ, 107, 1135
———. 1996, AJ, 112, 2300
White, S. M., Jackson, P. D., & Kundu, M. R. 1989, ApJS, 71, 895
Wilson, R. H. 1954, AJ, 59, 132
Worley, C. E. 1962, AJ, 67, 403
———. 1972, Publ. US Naval Obs., 22, Pt. 4
Worley, C. E., & Douglass, G. G. 1996, The Washington Visual Double Star Catalog, 1996.0 (Washington, DC: US Naval Obs.)